JOURNAL OF CATALYSIS **115**, 521–531 (1989)

Catalytic Reactions of *n*-Dodecane on Aluminosilicates

J. ABBOT AND B. W. WOJCIECHOWSKI

Chemical Engineering Department, Queen's University, Kingston, Ontario, Canada K7L 3N6

Received July 6, 1988; revised October 3, 1988

Catalytic reactions of *n*-dodecane at 400°C have been studied on HY, LaY, amorphous silica–alumina, HZSM-5, and H–mordenite. The molar distributions of initial products are almost identical on HY and LaY, while the distributions are shifted toward lower molecular weight products on the other catalysts. This we associate with initiation of cracking at Brønsted sites, which have higher acidities on amorphous silica–alumina, H–mordenite, and HZSM-5 than those present on HY and LaY. With the exception of HZSM-5, initial ratios of branched/linear paraffins are similar on all catalysts and show a preference for the branched isomer in the range C_4–C_8. On HZSM-5 the linear isomer is formed preferentially. This is attributed to restriction in the rearrangement of the carbonium ion in the narrower pores of the pentasil. The kinetic model previously applied to the cracking of linear paraffins on HY can also be applied to the cracking of *n*-dodecane on other aluminosilicate catalysts. The consequent kinetic parameters show that inhibition of the cracking reaction is greater on HY and LaY than on amorphous silica–alumina, H–mordenite, and HZSM-5. This is attributed to the stronger Lewis acidity of the carbenium ions formed by adsorption of product olefins at the stronger Brønsted sites on the later group of catalysts.

INTRODUCTION

There has been much recent interest in elucidating the details of the mechanism by which paraffins undergo cracking reactions on solid acid catalysts (*1–4*). As a result it has become increasingly clear that the protonation of saturated molecules at Brønsted sites to produce a carbonium ion plays an important role in the initiation of the cracking process. Many of the observed phenomena during reaction on solid acids at high temperatures parallel those in liquid superacids at low temperatures, where the involvement of carbocations has been well established (*5*).

We have previously discussed the cracking reactions of linear paraffins on HY in some detail (*2, 6*) and have concluded that the dominant mode of initiation is through the formation of carbonium ions at Brønsted sites. Analysis of product selectivity has shown that rearrangement of the linear carbonium occurs prior to cracking, which explains the appearance of branched paraffins as initial products. The kinetic model we have applied has also revealed that this cracking reaction is strongly inhibited by formation of product olefins (*7*). This has been associated with formation of carbenium ions at Brønsted sites. These, in turn, are much less effective in causing initiation through hydride ion abstraction or by proton insertion than the original sites on the inorganic surface.

These studies have now been extended to include the reaction of linear paraffins on other aluminosilicate catalysts. Reactions of *n*-dodecane on LaY, amorphous silica–alumina, H–mordenite, and HZSM-5 are reported here. It is interesting to note that a similar range of catalysts has recently been used in a study on the cracking of neopentane (*3*), where it was found that the dominant mode of cracking involved protolysis to yield methane and isobutene.

THEORY

Selectivity

For each reaction product, the time-averaged yield from $t = 0$ to t_f (the run duration)

0021-9517/89 $3.00

can be plotted against $\overline{X}_R$, the integral conversion of feed. Such plots can be enveloped by a single curve, the optimum performance envelope (OPE), which describes the selectivity behavior of a product as t_f approaches zero (*8*). This allows the source and subsequent behavior of products to be described by observing the morphology of the characteristic OPE curves which result. The initial selectivity of a product, given by the slope of the OPE at zero conversion, is nonzero for a primary product and zero for secondary and all subsequent products.

Kinetics

It has been shown (*7, 9*) that reactions of *n*-paraffins on HY can be described by

$$\frac{dX}{d\tau} = \frac{(1 + Gt)^{-N} A(1 - X)/(1 + \varepsilon X)}{1 + B(1 - X)/(1 + \varepsilon X)}, \quad (1)$$

where X is the fractional conversion of the paraffin, τ is the feed contact time, t is the time on stream, ε is the volume expansion coefficient, G and N are aging parameters, and A and B are constants related to the rate constant for reaction, and the Langmuir adsorption constants for reactant and products.

The constants A and B are defined by

$$A = \frac{\sum_i k_i K[C_0]}{1 + \sum_i K_j n_j [C_0]} \quad (2)$$

and

$$B = [C_0] \frac{K - \sum_j K_j n_j}{1 + \sum_j K_j n_j [C_0]}, \quad (3)$$

where k_i are the individual rate constants for the i parallel modes of conversion of the feed; K and K_j arre Langmuir adsorption constants for the feed C and each product P_j, respectively; n_j is a stoichiometric factor accounting for the number of product molecules of type j formed from the feed molecule; and $[C_0]$ is the initial concentration of reactant.

EXPERIMENTAL

The feedstocks were obtained from Aldrich and used without further purification. The purity of the *n*-dodecane used was 99.60%. The minor impurities present were isomers of the feedstock.

HY zeolite (97.3% exchanged) was prepared from NaY (Linde Co., Lot No. 45912, SK40) by repeated exchange with 0.5 *N* ammonium nitrate solution. LaY was prepared from the same NaY by repeated exchange with $La(NO_3)_3$ solution. H–mordenite was supplied by Strem Chemicals. HZSM-5 was synthesized according to procedures reported in the literature.

Catalysts were calcined at 500°C before use. All experiments were carried out using catalysts with mesh size 80/100. Reduction of the catalyst particle size and had no influence on the cracking reaction, showing that the reaction was not diffusion controlled.

All experiments were performed by using an integral, fixed-bed gas-phase plug flow reactor with an independently controlled three-zone heater. The experimental apparatus and procedures used were similar to those described in previous studies (*6*). All reactions were carried out at 400°C and 1 atm pressure.

Liquid products were analyzed by a Varian 6000 gas chromatograph with a 60-m SE-54 capillary column and flame ionization detection. Products up to C_7 were eluted at 35°C followed by a temperature program of 5°/min up to 300°C. Gaseous products were analyzed by a Carle SX1156 gas chromatograph. This enabled determination of all hydrocarbons in the range C_1–C_5, and the direct determination of hydrogen, if present. The identification of products was facilitated by use of a Finnigan 1020 automated GC/MS.

RESULTS AND DISCUSSION

Reaction on HY and LaY

Initial product selectivities for reactions of *n*-paraffins on HY have been reported previously (*6, 9*) and the initial fragmenta-

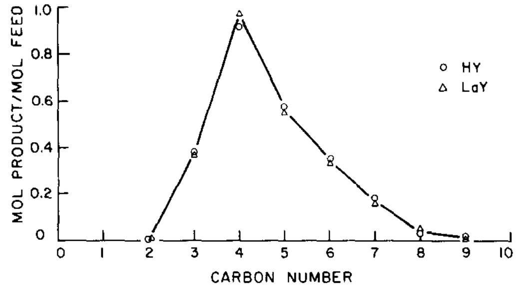

FIG. 1. Initial molar distributions of products formed on HY and LaY by reaction of *n*-dodecane at 400°C.

tion modes for *n*-dodecane on HY at 400°C have been analyzed in detail (*6*). Initial product selectivities for cracking of *n*-dodecane on HY at 400°C are given in Table 1, together with the corresponding results for reaction on LaY. The product selectivities are very similar on these two catalysts. This is illustrated in Fig. 1, where the initial molar product selectivities are plotted according to carbon number. The close correspondence in product distribution suggests that initiation of cracking occurs on very similar sites on these catalysts. The evidence strongly suggests that Brønsted sites (rather than Lewis sites) are dominant during initiation of cracking *n*-paraffins on HY (*2, 10, 11*). Cracking of the linear paraffin at a Brønsted site would occur through the formation of a carbonium ion, which can undergo cracking to yield a smaller paraffin and a residual carbenium ion. Brønsted sites are also present on LaY and are apparently formed from the hydrated form of the rare earth cation (*12, 13*). The relative proportions of Brønsted and Lewis sites on HY and LaY have been reported to differ significantly (*14, 15*). This supports the idea that only one type of site is active in this reaction, as a combination of contributing effects from two distinct types of site would be expected to depend on the ratio of their relative abundance. That, in turn, would not be expected to be the same in HY and LaY because of the differing acidity distributions caused by the two cations.

CRACKING ON HZSM-5, AMORPHOUS SILICA–ALUMINA, AND H-MORDENITE

Active Sites and Acidity

There now appears to be significant evidence to support the proposal that cracking of linear paraffins on HZSM-5 is initiated at Brønsted sites, through the initial formation of a carbonium ion (*1, 16*). A number of studies have concluded that there is a direct correlation between cracking activity of *n*-paraffins on HZSM-5 and the number of strong Brønsted sites (*17–19*). Infrared investigations have shown that the majority of Brønsted sites on HZSM-5 are highly acidic (*20*). Such methods show that these sites are more acidic than are the Brønsted sites on HY (*21*).

Both infrared (*22*) and NMR techniques (*23*) have shown that there is a strong similarity between the acidic OH groups present in amorphous silica–alumina and those in zeolites, although their concentration is much lower. Titration studies have indicated that the range of acidity in amorphous silica–alumina is much narrower than that in HY and is concentrated mainly in sites of high acidity (*24*). The broader range and heterogeneity of acidic sites in HY have been related to the lattice structure of the faujasite (*25*).

Infrared methods have also been used to investigate the acidity of H–mordenite (*26*), and both Brønsted and Lewis acid sites have been identified. As in the case of HY, it has been demonstrated that cracking activity for *n*-paraffins is decreased as the pretreatment temperature for H–mordenite is increased (*10*). The effect can be reversed by addition of water, which constitutes strong evidence in support of the proposal that it is the Brønsted sites that are active in the cracking process. It has been suggested that the Brønsted sites on H–mordenite are of higher acidity that those on HY (*27*), possibly resulting from an interaction between the hydroxyl groups and Lewis acid centers through an inductive mechanism.

TABLE 1

Initial Selectivities[a] for Reaction of *n*-Dodecane on Acid Catalysts at 400°C

Product	Initial weight selectivity					
	HY	LaY	Amorphous SiAl	H-mordenite	HZSM-5 (I)	HZSM-5 (II)
Methane	0	0	0	0	0	0
Ethane	0	0	0	0	0	0
Ethylene	0	0	0.0061	0.0143	0.011	0.0095
Propane	0.0180	0.020	0.061	0.062	0.072	0.0764
Propylene	0.0753	0.0750	0.1365	0.118	0.164	0.165
n-Butane	0.0321	0.0370	0.0454	0.0490	0.0967	0.0928
Isobutylene	0.0753	0.0836	0.108	0.140	0.0310	0.0349
trans-2-Butene	0.0527	0.049	0.0583	0.0564	0.0533	0.0547
cis-2-Butene	0.0316	0.035	0.0398	0.0382	0.0355	0.0387
Isobutene	0.1205	0.090	0.139	0.139	0.1582	0.147
n-Pentane	0.0210	0.023	0.0153	0.0210	0.0774	0.0736
2-Methylbutane	0.0853	0.0856	0.0641	0.0620	0.0129	0.00883
trans-2-Pentene	0.0231	0.022	0.0183	0.0164	0.0182	0.0210
cis-2-Pentene	0.0140	0.0110	0.0098	0.00905	0.0114	0.0123
3-methyl-1-Butene	0	0.00304	0.0037	0.00308	0.0044	0.0042
2-methyl-1-Butene	0.0271	0.0220	0.0256	0.0256	0.0244	0.0297
2-methyl-2-Butene	0.0597	0.0551	0.0623	0.0634	0.0692	0.0784
1-Pentene	0.0073	0.0065	0.00533	0.00514	0.00732	0.00629
n-Hexane	0.0210	0.0201	0.0133	0.0130	0.0372	0.0352
2-Methylpentane	0.0452	0.0465	0.0220	0.0168	0.0047	0.0041
3-Methlpentane	0.0228	0.0259	0.0141	0.00834	0.00146	0.00120
2, 3-Dimethylbutane	0	0.0088	0.0070	0.00284	0	0
C_6 olefins	0.0916	0.0710	0.0732	0.0808	0.0768	0.0810
n-Heptane	0.0110	0.0140	0.00531	0.0060	0.0144	0.0131
2-Methylhexane	0.0251	0.0230	0.00799	0.00558	0	0
3-Methylhexane	0.0191	0.0240	0.00666	0.00295	0	0
2, 3-Dimethylpentane	0.0073	0.00855	0.00221	0	0	0
2, 4-Dimethylpentane	0.0085	0	0	0	0	0
C_7 olefins	0.0339	0.0229	0.0221	0.00753	0.0051	0.00569
n-Octane	0	0.0090	0.00312	0.00363	0.0120	0.0102
2-Methylheptane	0.0080	0.0149	0.00155	0.00291	0	0
3-Methylheptane	0.0091	0.0101	0.00194	0.00154	0	0
4-Methylheptane	0	0	0	0	0	0
2, 3-Dimethylhexane	0	0	0	0	0	0
2, 4-Dimethylhexane	0	0	0	0	0	0
2, 5-Dimethylhexane	0	0.0030	0	0	0	0
Toluene	0	0	0	0.0021	0	0
C_8 aromatics	0	0.0038	0.00412	0.0026	0	0
C_9 aromatics	0	0.0070	0.00163	0	6	6
C_9 paraffins–olefins	0	0	0	0.0067	0.0047	0.0035
C_{10} aromatics	0	0	0	0	0	0
$C_{10} + C_{11}$ paraffins	0	0	0	0	0	0
C_{12} (skeletal isomerization)	0.0361	0.0600	0	0	0	0
Coke	0.0169	0.0165	0.0100	0.0130	0.0025	0.0020
Total	0.9987	1.0068	0.9946	0.999	1.005	1.009

---

[a] Initial selectivities were obtained by taking initial slopes of optimum performance envelopes (see Figs. 2 and 3).

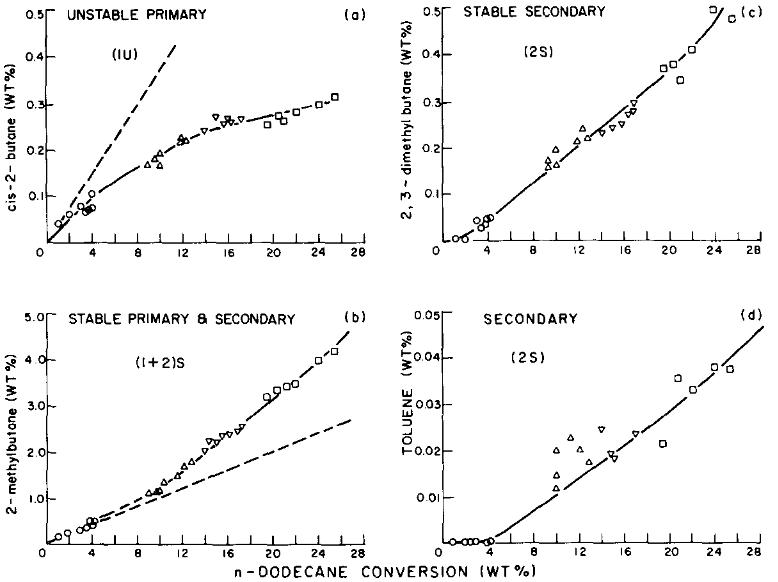

FIG. 2. Optimum performance envelopes for products of cracking *n*-dodecane on HY at 400°C. (a) *cis*-2-Butene, (b) 2-methylbutane, (c) 2,3-dimethylbutane, (d) toluene. Catalyst-to-reactant ratios: (○) 0.0033, (△) 0.0333, (▽) 0.0655, (□) 0.1400. Dashed lines show initial selectivity.

Product Selectivity

The initial product selectivities for reaction of *n*-dodecane at 400°C on HZSM-5, H-mordenite, and amorphous silica–alumina are given in Table 1. As for reaction on HY and LaY, initial selectivities were determined from initial slopes of optimum performance envelopes. This method is superior to examination of product distribution at some arbitrary conversion level, as it makes it possible to distinguish unambiguously between primary and secondary products. This is illustrated for several products of reaction of *n*-dodecane on HY at 400°C in Fig. 2. It is clear that this figure that toluene is a secondary product, whereas a single experiment at, say, 10% conversion would not allow this identification to be made. Figure 3 shows optimum performance envelopes for isobutane formation on each catalyst, illustrating how the initial selectivity values in Table 1 were obtained. On all catalysts reported here, the major products from cracking are acylic paraffins and olefins. The formation of aromatics and coke contributes only in small measure to the total initial selectivities.

Figure 4 shows initial product distributions according to carbon number for reaction on HZSM-5, H-mordenite, and amorphous silica–alumina. It is clear that each of these distributions is shifted relative to the corresponding profile for initial reaction on HY, reflecting a higher probability for the formation of lower molecular weight fragments. It is also apparent that the initial product distributions by carbon number observed from cracking *n*-dodecane are very similar on these three catalysts. This type of shift in product distribution has been reported previously for comparative cracking studies of *n*-hexadecane on amorphous silica–alumina and HY (*28–30*), and for HZSM-5 and HY using *n*-heptane (*31*), and a mixed paraffin feedstock (*32*).

Methane and molecular hydrogen were not observed as initial products for reaction of *n*-dodecane at 400°C on any of the catalysts studied. It has recently been reported (*3*) that hydrogen could not be detected during reaction of neopentane on these cat-

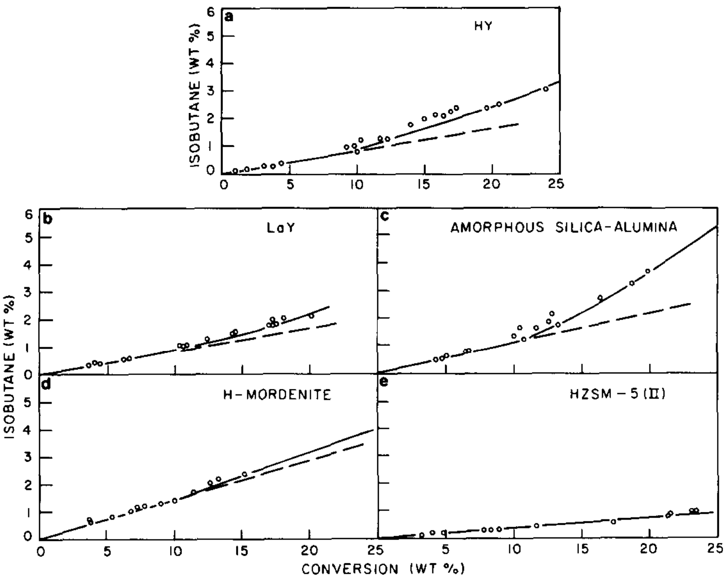

FIG. 3. Optimum performance envelopes for formation of isobutane from reaction of *n*-dodecane at 400°C on (a) HY, (b) LaY, (c) amorphous silica–alumina, (d) H-mordenite, (e) HZSM-5 (II). Dashed lines show initial selectivities.

alysts at 400–500°C, and we were unable to detect hydrogen for reaction of *n*-dodecane at any level of conversion studied.

The absence of hydrogen and methane must not be taken as evidence to suggest that nonclassical carbonium ion intermediates are not formed. Haag and Dessau have reported that these products are observed for reaction of C_6 paraffins on HZSM-5 (*1*). However, this does not mean that these species are the necessary indicator for this type of intermediate. Extensive studies by Olah and co-workers (*5*) clearly show that for reaction in liquid superacids, where the concepts of these types of carbocations originated, the product distributions observed depend strongly on the molecular structure of the hydrocarbon.

For example, the major products formed during cracking of *n*-octane are C_3, C_4, and C_5. The rupture of the C–H bond (to produce molecular hydrogen) is not favored for this *linear* paraffin—nor is cleavage of the terminal C–C bond to form methane.

If it is assumed that the cracking reaction on each of the aluminosilicate catalysts is initiated by the same mechanism, namely protonation of the paraffin at Brønsted sites, it appears reasonable to suggest a relationship between the observed initial fragmentation distribution and acid strength of the active sites on the catalysts. Cracking on sites of higher acidity should lead to smaller product fragments. A number of studies have shown that C–C bonds become more resistant to cracking progressing from the center of a linear paraffin toward the terminal bonds (*2*, *33*). Thus, there is a higher probability of producing the small C_2 and C_3 fragments for reaction on catalysts such as HZSM-5 and amorphous silica–alumina where the acidity is higher than that on HY. This explanation has also been suggested to account for the initial product distributions from *n*-hexadecane and hexadecene on HY at 400°C (Fig. 3), where it was postulated (*34*) that cracking occurred at Brønsted sites in both cases, but initial formation of the C_{16} carbenium ion by adsorption of the olefin occurred over a broader range of site acidity.

Initiation of cracking of a linear paraffin

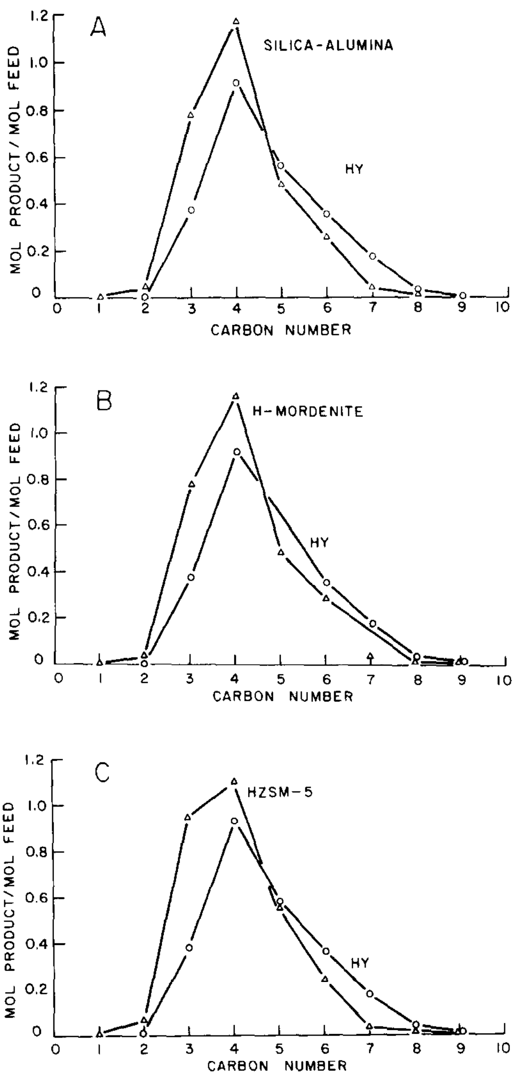

FIG. 4. Initial molar distributions of products formed on amorphous silica–alumina, HZSM-5, and H–mordenite by reaction of *n*-dodecane at 400°C.

at a Brønsted site via protonation leads to a carbonium ion, which can subsequently crack to produce a smaller saturated molecule and an adsorbed carbenium ion. Rearrangement of the protonated species prior to cracking has been suggested to account for the appearance of branched paraffins as initial products from reaction of *n*-alkanes on HY (*2*, *32*), rather than assuming that Lewis acid sites are dominant during the initiation process (*35*). Table 2 gives initial ratios of branched/linear paraffins formed from *n*-dodecane on each catalyst. It is apparent that these ratios are very similar at each carbon number for reaction on HY, and LaY, and amorphous silica–alumina. This would appear to be unlikely if branched paraffins were formed initially only at Lewis sites, as it would imply that the ratio of Brønsted to Lewis sites active in the cracking reaction is the same on each catalyst. Any correlation between this ratio and the relative proportion of sites (*35*) appears dubious, particularly in view of the close similarity of products on HY and LaY, where the proportion of Brønsted and Lewis acid site differs significantly (*14*, *15*).

Table 2 also shows that the ratio of branched/linear paraffins initially produced is somewhat reduced in the sequence HY–LaY–Si/Al–H-mordenite. It is significantly lower at each carbon number for reaction on HZSM-5. This we attribute to the increasing difficulty in rearrangement of the protonated species, as the pore size of the catalyst approaches the kinetic diameter of a branched alkane (*36*).

Table 3 gives the initial ratios of branched/linear olefins at C_4 and C_5 for reaction of *n*-dodecane on each catalyst. In contrast to paraffin formation, it is apparent that these ratios are little influenced by the structure of the catalyst, showing that carbenium ion rearrangement is not restricted (*32*).

Kinetics of Cracking Reactions

Figure 5 shows theoretical curves obtained by fitting experimental points by Eq. (1), for reactions of *n*-dodecane at 400°C on HY, LaY, H-mordenite, amorphous silica–alumina, and HZSM-5. Table 4 gives values for the optimum kinetic parameters obtained. The values of the expansion factor ε are calculated from initial selectivities, and it can be seen that this factor increases for the reaction on silica–alumina, H–mordenite, and HZSM-5 where the fragmentation distribution is shifted to products of lower carbon number.

TABLE 2

Ratios of Branched/Linear Paraffins Initially Produced from Reaction of *n*-Dodecane at 400°C

Carbon number	Catalyst					
	HY	LaY	Amorphous Si/Al[a]	H-mordenite	HZSM-5 (I)[b]	HZSM-5 (II)[b]
4	2.3	2.3	2.4	2.9	0.32	0.38
5	4.1	3.7	4.2	3.0	0.17	0.12
6	3.2	4.0	3.2	2.2	0.17	0.15
7	5.5	4.0	3.2	1.4	0	0
8		2.8	1.1	1.2	0	0

[a] The SiO_2/Al_2O_3 ratio of the Si/Al was 4.

[b] The SiO_2/Al_2O_3 ratio of HZSM-5 (I) was 60. The SiO_2/Al_2O_3 ratio of HZSM-5 (II) was 124.

Inhibition and Extent of Chain Reactions

It has previously been reported that reaction of *n*-paraffins on HY in the range 400–500°C is strongly inhibited by the formation of product olefins (*2, 7*). This can be deducted from the value of the parameter B, which approaches -1 when the cracking reaction is strongly inhibited (Table 4). The reasons for this have previously been discussed in terms of the Langmuir adsorption constants for the reactant (K) and products (K_j). From Eq. (3), it follows that B approaches -1 when $K \ll \Sigma K_j n_j$, under the condition $1 \ll \Sigma K_j n_j [C]_0$ (*7*). Table 4 shows that B is also close to -1 for reaction of *n*-dodecane at 400°C on LaY, which is another indication that the active sites on HY and LaY are very similar.

For reaction on HZSM-5, silica–alumina, and H-mordenite, however, parameter B falls in the range -0.6 to -0.8. This reflects a reduction in the degree of inhibition, which can be explained by asserting that there is less difference in the magnitudes of K and $\Sigma K_j n_j$ on these catalysts. We note that the relationships between adsorption constants for reactant and products in Eq. (3) are based on the assumption that the adsorption of a product molecule at a Brønsted site renders that site inactive with regard to cracking the feed until a desorption occurs. However, adsorption of a product olefin produces a carbenium ion, which itself could in some cases initiate cracking of the feed by acting as a Lewis site. This comes about because if the carbenium ion is a sufficiently strong Lewis acid, it will abstract a hydride ion from the feed, producing a paraffin and a new carbenium ion derived from the feed molecule and, in this way, give rise to a chain process. This in turn will lower or even eliminate the inhibition caused by the adsorption of products on the original active sites of the catalyst.

Molecular orbital calculations have

TABLE 3

Ratios of Branched/Linear Olefins Initially Produced by Reaction of *n*-Dodecane at 400°C

Carbon number	Catalyst					
	HY	LaY	Amorphous Si/Al	H-mordenite	HZSM-5 (I)	HZSM-5 (II)
4	1.4	1.1	1.4	1.5	1.8	1.6
5	2.0	2.0	2.7	3.0	2.6	2.8

TABLE 4

Kinetic Parameters for Reaction of *n*-Dodecane HY at 400°C

Catalyst	A (mol/g cat./min)	B	N	G (min^{-1})	m	k_{md} (min^{-1})	ε
HY	0.66	−0.99	0.88	1.43	2.1	1.30	1.30
LaY	1.06	−0.98	0.72	9.09	2.4	6.5	1.30
Amorphous Si/Al	0.013	−0.80	161	0.0004	1.0	0.065	1.83
H–mordenite	0.91	−0.63	0.34	9.81	3.9	3.4	1.90
HZSM-5 (II)	6.83	−0.79	0.79	178	13.7	14.0	1.90

shown that cracking of *n*-heptane via protonation is energetically more favorable than that through hydride ion abstraction (*37*). This would lead us to conclude that the carbenium ions formed by olefin adsorption at Brønsted sites on HZSM-5, silica–alumina, and H–mordenite are stronger Lewis acids than their counterparts on HY, suggesting in turn that their Lewis acidity is directly related to the strength of the original Brønsted site. The new cracking sites, the carbenium ion based Lewis sites, will decay precisely in the same way as the original Brønsted sites since they are on the original Brønsted sites. However, the selectivity on such sites may be different than the initial selectivity obtained on the fresh catalyst when no such carbenium ion Lewis sites were present.

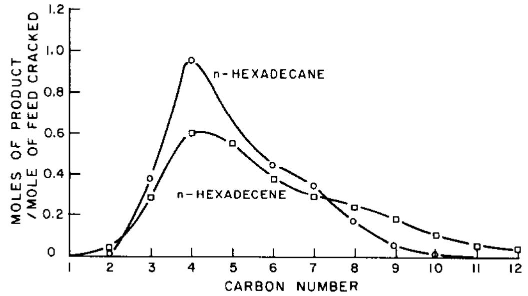

FIG. 5. Initial molar distributions of products formed on HY at 400°C from reaction of *n*-hexadecane and hexadecene.

Catalyst Decay

According to the time on stream theory (*38*), the rate of loss of active sites is given by

$$\frac{d\theta}{dt} = k_{md}\,\theta^{m}, \qquad (4)$$

where θ is the fraction of active sites remaining at time t, k_{md} is the deactivation rate constant, and m is the order of decay. Values of k_{md} and m have been calculated from values of the parameters G and N (*9*) and are shown in Table 4. For reaction of *n*-paraffins on HY the order of decay is ~2. This order has also been observed for reaction of other feedstocks on this catalyst, including cumene (*39*) and olefins (*40*). This has been interpreted as indicating a decay process which involves two active sites per decay event. Values of m larger than 2 are found when there is also some contribution from pore blocking to the process of deactivation (*31*).

Table 4 shows that the order of deactivation during reaction of *n*-dodecane at 400°C on LaY is also ~2. However, the orders of decay on the other catalysts studied are significantly different. The very high order of decay observed on HZSM-5 (m = 13.7) is consistent with pore blocking as the dominant mechanism leading to loss of activity. High orders of decay have previously been reported for reaction of cumene on HZSM-5 (*41*). The order of decay on H–mordenite

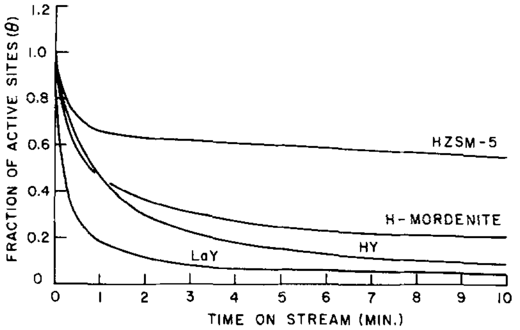

FIG. 6. Fraction of active sites remaining (θ), plotted as a function of time for HZSM-5, H-mordenite, HY, and LaY during reaction of *n*-dodecane at 400°C.

($m = 3.9$) also suggests that pore blockage is important on this catalyst, where the pore dimensions are intermediate between those in the large-pore zeolite HY and those on HZSM-5.

On amorphous silica–alumina, the value of the decay exponent is 1.0, indicating the loss of only one active site per decay event. Amorphous silica–alumina is generally reported to have significantly lower activity than HY zeolite. This is confirmed by comparing values of A in Table 4, which are directly proportional to the sum of rate constants Σk_i. This can be related to the much lower density of Brønsted sites on silica–alumina mentioned earlier. The observed order of decay on this catalyst can also be attributed to this low site density. Loss of more than one site per decay event would require that such sites be located within some critical distance of one another. On silica–alumina, the Brønsted sites active in cracking are sparsely distributed, so that it becomes improbable that more than one site is eliminated in a single decay event.

Using the integrated form of Eq. (3), it is possible to plot the fraction of active sites remaining as a function of time. This is illustrated in Fig. 6. It can be seen that deactivation occurs more slowly on HZSM-5 than on HY (*42*, *43*). This can be attributed to the smaller pore dimensions within the pentasil (*36*). Our model shows that the rate of deactivation of H-mordenite is intermediate between HY and HZSM-5, being closer to that of HY. This sequence also appears to follow the pattern established for ratios of branched/linear paraffins in terms of pore size dimensions. There have been reports that H-mordenite is particularly susceptible to coke formation and deactivation during cracking (*3*). However, some of these studies can be misleading as experiments using H-mordenite were carried out at significantly lower temperatures than those used for HY or HZSM-5 (*3*). Our studies with *n*-hexadecane (*9*) clearly show that the nature of coke deposited during cracking is a strong function of temperature and that coke is more highly dehydrogenated at low temperatures.

CONCLUSION

Cracking seems to be initiated at Brønsted sites through the formation of a carbonium ion in each case. Initial product distributions on HY and LaY are very similar, but shifted in favor of lower molecular weight products on the other catalysts studied. This has been attributed to the presence of Brønsted sites of higher acidity on amorphous silica–alumina, H-mordenite, and HZSM-5. The ratios of branched/linear paraffins initially produced are similar on each catalyst, with the exception of HZSM-5 where it is much lower. This is attributed to the influence of pore structure which prevents the branching of carbonium ions but has little effect on the branching of carbenium ions.

Application of a kinetic model to the cracking of *n*-dodecane on aluminosilicates shows that the reaction is less inhibited by product formation during reaction on amorphous silica–alumina, H-mordenite, and HZSM-5 than the reaction on HY or LaY. This suggests that the carbenium ions generated through the adsorption of product olefins may be effective in these cases as Lewis sites which participate in a chain reaction via hydride transfer. These sites, it seems, are active only when they are produced from catalysts having strong Brønsted sites. The kinetic model also shows characteristic distinctions in the aging behavior of different structural classes of catalyst. Two-site decay has been observed for the faujasites. One-site decay is observed on amorphous silica–alumina. This can be attributed to the low site density on that material. High orders of decay on H–mordenite and in particular on HZSM-5 can be understood as a consequence of their narrower pore dimensions which are readily plugged by the formation of large molecular species frequently associated with coke.

Overall, it seems that the same general mechanism is operating on each catalyst. Differences which appear in product selectivity and kinetic phenomena can all be explained in terms of differences in the distributions of Brønsted acid site strength and by steric effects due to catalyst structure.

ACKNOWLEDGMENTS

We thank the Natural Sciences and Engineering Research Council of Canada and Queen's University Advisory Research Committee for financial support.

REFERENCES

1. Haag, W. O., and Dessau, R. M., "Proceedings, 8th International Congress on Catalysis, Berlin, 1984," Vol. II, p. 305. Dechema, Frankfort am Main, 1984.
2. Abbot, J., and Wojciechowski, B. W., *J. Catal.* **115,** 1 (1988).
3. Lombardo, E. A., Pierantozzi, R., and Hall, W. K., *J. Catal.* **110,** 171 (1988).
4. Weitkamp, J., Jacobs, P. A., and Martens, J. A., *Appl. Catal.* **8**(1), 123 (1983).
5. Olah, G. A., Halpern, Y., Shen, J., and Mo, Y. K., *J. Amer. Chem. Soc.* **95,** 4960 (1973).
6. Abbot, J., and Wojciechowski, B. W., *J. Catal.* **107,** 451 (1987).
7. Abbot, J., and Wojciechowski, B. W., *J. Catal.* **104,** 80 (1987).
8. Ko, A. N., and Wojciechowski, B. W., *Prog. React. Kinet.* **12,** 201 (1983).
9. Abbot, J., and Wojciechowski, B. W., *J. Catal.* **109,** 274 (1988).
10. Benesi, H. A., *J. Catal.* **8,** 368 (1967).
11. Hopkins, P. D., *J. Catal.* **12,** 325 (1968).
12. Moscou, L., and Lakeman, M., *J. Catal.* **16,** 173 (1976).
13. Venuto, P. B., Hamilton, L. A., and Landis, P. S., *J. Catal.* **5,** 484, (1964).
14. Corma, A., Fornes, V., Monton, J. B., and Orchilles, A. V., *Appl. Catal.* **12,** 105 (1984).
15. Corma, A., Farag, H., and Wojciechowski, B. W., *Int. J. Chem. Kinet.* **13,** 883 (1981).
16. Sendoda, Y., and Ono, Y., *Zeolites* **8,** 101 (1988).
17. Borade, R. B., Hedge, S. G., Kulkasni, S. B., and Ratnasamy, *Appl. Catal.* **13,** 27 (1984).
18. Haag, W. O., Lago, R. M., and Weisz, P. B., *Nature (London)* **309,** 589 (1984).
19. Klyachko, A. L., Kapustin, G. I., Brueva, T. R., and Rubinstein, A. M., *Zeolites* **7,** 119 (1987).
20. Datka, J., and Piwowarska, Z., *Zeolites* **8,** 30 (1988).
21. Hedge, S. G., Ratnasamy, P., Kustov, L. M., and Kazansky, V. B., *Zeolites* **8,** 137 (1988).
22. Borovkov, V. Y., Alexeev, A. A., and Kazansky, V. B., *J. Catal.* **80,** 462 (1983).
23. Liang, S. H. C., and Gay, I. D., *J. Catal.* **66,** 294, (1980).
24. Otouma, H., Yoshimasa, A., and Uhihashi, H., *Bull. Chem Soc. Japan* **42,** 2449 (1969).
25. Mikovsky, R. J., and Marshall, J. F., *J. Catal.* **44,** 170 (1976).
26. Lefrancois, M., and Malbois, G., *J. Catal.* **20,** 350 (1971).
27. Benesi, H. A., and Winquist, B. H. C., "Advances in Catalysis," Vol. 27, p. 97. Academic Press, New York, 1987.
28. Bartley, B. H., and Emmett, P. H., *J. Catal.* **89,** 442 (1984).
29. Bordley, J. L., and Emmett, P. H., *J. Catal.* **42,** 367 (1976).
30. Nace, D. M., *Ind. Eng. Chem.* **8**(1), 31 (1969).
31. Corma, A., Monton, J. B., and Orchilles, A. V., *Appl. Catal.* **16,** 59 (1985).
32. Abbot, J., and Wojciechowski, B. W., *Ind. Eng. Chem. Prod. Res. Dev.* **24,** 501 (1985).
33. Coonradt, H. L., and Gaswood, W. E., *Ind. Eng. Chem. Process Des. Dev.*, 38 (1964).
34. Abbot, J., submitted for publication.
35. Corma, A., Planelles, J., and Tomas, F., *J. Catal.* **94,** 445 (1985).
36. Ruthven, M., *Chem. Eng. Prog.* **84**(2), 42 (1988).
37. Corma, A., Planelles, J., Sanchez-Maris, J., and Tomas, F., *J. Catal.* **93,** 30 (1985).
38. Wojciechowski, B. W., *Catal. Rev. Sci. Eng.* **9**(1), 79 (1974).
39. Corma, A., and Wojciechowski, B. W., *Catal Rev. Sci. Eng.* **24**(1), 1 (1982).
40. Abbot, J., and Wojciechowski, B. W., *J. Catal.* **108,** 346 (1987).
41. Fukase, S., and Wojciechowski, B. W., *J. Catal.* **109,** 180 (1988).
42. Hammon, V., Kokotailo, G. T., Riekert, L., and Zhou, J. Q., *Zeolites* **8**(4), 330 (1988).
43. Rollmann, L. D., and Walsh, D. E., *J. Catal.* **56,** 139 (1979).
44. Walsh, D. E., and Rollmann, L. D. *J. Catal.* **56,** 195 (1979).